

Magnetization oscillation in a nanomagnet driven by a self-controlled spin-polarized current: Nonlinear stability analysis

Xiao Chen,¹ Zhizhuai Zhu,¹ Yun Jing,² Shuai Dong,¹ and Jun-Ming Liu^{1,3,*}

¹Laboratory of Solid State Microstructures, Nanjing University, Nanjing 210093, China

²Department of Electronic Science and Engineering, Nanjing University, Nanjing 210093, China

³International Center for Materials Physics, Chinese Academy of Sciences, Shenyang 110015, China

(Received 25 June 2007; published 7 August 2007)

The magnetization dynamics of a nanomagnet is investigated by performing macromagnetic simulation and nonlinear stability analysis on the spin precession trajectory. We propose a scheme in which a self-controlled spin-polarized current plus a magnetic field is employed to excite the self-oscillation of the magnetization through spin precession. It is revealed that the negative feedback mechanism of the spin torque is responsible for the self-oscillation excitation. The periodic solutions and the limit cycle stability for two specific configurations in terms of the directions of the spin-polarized current and magnetic field are analyzed, implying that the self-oscillation of magnetization essentially depends on the demagnetization field.

DOI: 10.1103/PhysRevB.76.054414

PACS number(s): 75.75.+a, 75.60.Jk, 75.40.Gb, 85.70.Ay

I. INTRODUCTION

A spin-polarized current (hereafter referred to as SP current), when passing through a magnet, will transfer a spin angular momentum to the magnet.^{1,2} This angular momentum transfer can be understood in terms of spin precession (say, magnetization reversal) induced by a spin torque. Recently, significant efforts have been directed toward the understanding of the physics underlying the spin torque effect³⁻⁵ because the ultrafast reversal and highly stable time oscillation of the magnetization are of significant importance for related potential applications.⁵⁻¹² Currently, the spin torque induced magnetization reversal in a nanomagnet by employing the SP current seems to be an efficient and controllable way.⁵ The spin torque generated by the SP current is fundamentally different from the torque generated by an external magnetic field. It neither directly influences the spin precession of the nanomagnet nor dissipates the energy, and thus can be either an energy source or sink.

Based on this feature, the spin torque can lead to some interesting magnetization behaviors in the nanomagnet when the SP current is applied along a special direction.⁹ Among these behaviors, the stable oscillation of magnetization represents the most intriguing effect.¹³⁻¹⁹ Recently, Bertotti *et al.* thoroughly analyzed the stability diagram of the magnetization dynamics dominated by a modified Landau-Lifshitz-Gilbert (LLG) equation in the state space of a magnetic field and the SP current. They predicted the existence of self-oscillation solutions in some regions of the state space.¹³ In these regions, Rippard *et al.* demonstrated that the spin precession can be synchronized with a small alternating SP current of frequency f imposed onto a direct SP current (phase locking).¹⁵ However, these studies, typically employing the SP current approach, focused on excitation of magnetic oscillation by means of varying the dc or radio frequency current pulses. This kind of oscillation may not last for a long time in practice due to the noise and damping effects.

In this paper, we propose a scheme to excite the self-oscillation of magnetization in a nanomagnet by injecting a SP current which is self-controlled with the magnetization. In

fact, the self-control is a popular technique extensively employed in many fields, such as biomedical engineering. Recently, Sun and Wang²⁰ and Thirion *et al.*²¹ proposed a scheme for self-controlling the magnetic field in order to switch the magnetization of a nanomagnet and predicted that the time for magnetization switching can be dramatically reduced compared with that under a dc magnetic field. We shall report that the self-oscillation of magnetization is highly stabilized by means of a self-controllable SP current. This self-oscillation results from the negative feedback effect of the spin torque induced by the self-controlled SP current and is qualitatively different from the self-oscillation behavior discussed earlier.^{13,15} More detailed investigation indicates that this self-oscillation can be easily manipulated by a proper combination of the SP current and magnetic field. The stability of the self-oscillation depends essentially on the demagnetization field of the nanomagnet under consideration. We argue that this scheme represents an effective approach to generate and modulate the highly stable self-oscillation of magnetization in nanomagnets and may find potential applications in the manipulation of some nanoscale devices such as microwave sources and resonators.

II. MODEL AND STABILITY ANALYSIS

A. Model

We start from a single-domain nanomagnet and assume that the spin dynamics can be described by the LLG equation with an additional spin torque term induced by the SP current S . The motion of magnetization vector \mathbf{M} follows^{20,22}

$$\frac{1 + \alpha^2}{\gamma} \frac{d\mathbf{M}}{dt} = -\mathbf{M} \times \mathbf{h}_{\text{eff}} - \frac{\alpha}{M_s} \mathbf{M} \times (\mathbf{M} \times \mathbf{h}_{\text{eff}}) - \frac{1}{M_s} \mathbf{M} \times (\mathbf{M} \times \mathbf{S}). \quad (1)$$

The motion of the dimensionless magnetization vector \mathbf{m} with $|\mathbf{m}|=1$ follows^{20,22}

$$\frac{1 + \alpha^2}{\gamma} \frac{d\mathbf{m}}{dt} = -\mathbf{m} \times \mathbf{h}_{\text{eff}} - \alpha \mathbf{m} \times (\mathbf{m} \times \mathbf{h}_{\text{eff}}) - \mathbf{m} \times (\mathbf{m} \times \mathbf{S}), \quad (2)$$

where $\mathbf{m} = \mathbf{M}/M_s$, M_s is the saturation magnetization, t is the time, α is the damping coefficient ($\alpha=0.01$), γ is the gyromagnetic ratio ($\gamma=1.7 \times 10^7 \text{ Oe}^{-1} \text{ s}^{-1}$); \mathbf{h}_{eff} is the effective field vector, and $\mathbf{S} = S\mathbf{e}_p$ represents the SP current field with magnitude S and unit vector \mathbf{e}_p defining the spin polarization direction,²³ both of which will be self-controlled with \mathbf{m} . Equation (2) can be further written into a completely dimensionless form for convenience of mathematical analysis. However, we still use Eq. (2) for numerical processing below so that the values of the effective field components and SP current are given in the unit of oersted for practical convenience.

The effective field $\mathbf{h}_{\text{eff}} = (h_x, h_y - h_k m_y, h_z - h_{de} m_z)$, with external magnetic field $\mathbf{h}_{\text{ex}} = (h_x, h_y, h_z)$, magnetic anisotropy field h_k in the y direction ($h_k=500 \text{ Oe}$ is taken), and demagnetization field h_{de} along the z axis ($h_{de}=5000 \text{ Oe}$). The values of these parameters are chosen, referring typically to Permalloy nanomagnets.^{5,13,14} Each component of \mathbf{h}_{eff} generates a torque acting on \mathbf{m} . We denote the torques induced by \mathbf{h}_{ex} , h_{de} , h_k as Γ_1 , Γ_2 , Γ_3 , respectively, noting that Γ_2 always pulls \mathbf{m} onto the x - y plane and $\Gamma_2 \gg \Gamma_3$. We mainly investigate the effect of Γ_2 on the oscillation behavior of \mathbf{m} because Γ_3 is not significant, noting $h_k/h_{de}=0.1$, and even though all of these torque terms are included in the calculation.²² The free energy of the magnet can be defined as

$$E = \frac{1}{2} h_k m_y^2 + \frac{1}{2} h_{de} m_z^2 - \mathbf{h}_{\text{ex}} \cdot \mathbf{m}, \quad (3)$$

B. Stability analysis

Equation (2) allows us to argue that a stable oscillation of \mathbf{m} with time t may not be possible unless a delicate balance between torques Γ_1 , Γ_2 , Γ_3 and the torque generated by \mathbf{S} is maintained. Equation (2) is a nonlinear ordinary differential equation which is solved numerically by adopting the fourth-order Runge-Kutta algorithm, as usually done.²² In addition, we analyze the stability of the spin precession over the (θ, φ) state space, where θ is the polar angle and φ is the azimuthal angle (see Fig. 1), noting that the nanomagnet is assumed to be a macrospin.

According to the Poincare-Bendixson theorem, if the macrospin motion proceeds in the (θ, φ) state space and is limited within a finite-size region, there are only two types of motion trajectory upon time $t \rightarrow \infty$: the trajectory approaches either a fixed point or a limit cycle. No chaotic trajectories can be possible.²⁴ It is possible to excite the self-oscillation of \mathbf{m} by applying a static dc field $\mathbf{h}_{\text{ex}} = (h_x, h_y, h_z)$ in combination with a self-controlled \mathbf{S} . For this purpose, extensive calculation of the trajectories of \mathbf{m} over the entire (θ, φ) state space is performed to search for the scheme with which the self-controlling of \mathbf{S} with \mathbf{m} can be realized, so that the self-oscillation of \mathbf{m} retains long-time high stability. Figure 1

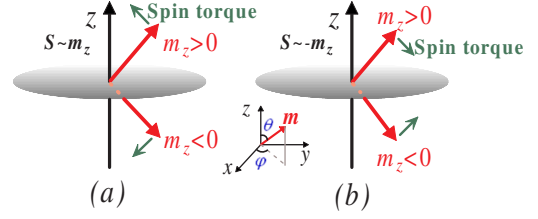


FIG. 1. (Color online) A schematic of spin torque caused by the self-control current. (a) $\mathbf{S} = S_0 \mathbf{m}_z$; spin torque will draw the nanomagnet to the $+z$ axis if $m_z > 0$, otherwise it will pull the nanomagnet to the $-z$ axis. (b) $\mathbf{S} = S_0 (-\mathbf{m}_z)$; spin torque will try to sustain the nanomagnet on the x - y plane.

shows a schematic drawing of the spin torque [green (gray) arrows] imposed to the nanomagnet in two different manners. In Fig. 1(a), \mathbf{S} is modulated according to $\mathbf{S} \propto \mathbf{m}_z$, where m_z is the z axis component of \mathbf{m} . The spin torque generated by \mathbf{S} will enforce \mathbf{m} toward the z axis. If \mathbf{h}_{ex} is applied along the x axis, \mathbf{m} will exhibit the self-oscillation in the y - z plane. We refer to this self-oscillation as mode I, where \mathbf{S} is always perpendicular to \mathbf{h}_{ex} so that the spin torque, as the negative feedback effect, reaches the maximum and maintains the highly stable oscillation of \mathbf{m} . In Fig. 1(b), $\mathbf{S} \propto -\mathbf{m}_z$ is conducted so that \mathbf{m} eventually aligns onto the x - y plane. If \mathbf{h}_{ex} is applied along the z axis, a self-oscillation of \mathbf{m} of high stability in the x - y plane will be reached. We refer to this self-oscillation as mode II, where \mathbf{S} is always parallel to \mathbf{h}_{ex} so that the negative feedback effect reaches the maximum, too, for the highly stable oscillation of \mathbf{m} .

It should be mentioned that the two modes of self-oscillation remain quite stable even if damping coefficient α fluctuates over a broad range as long as the magnitude of \mathbf{S} is appropriately chosen, indicating that the two modes can be utilized for manipulating nanomagnets of different damping behaviors. In addition, the above discussion applies identically to the cases where \mathbf{h}_{ex} applies along the $\pm x$ axis (mode I) or $\pm z$ axis (mode II).

In the following, we will investigate in detail the self-oscillation behaviors of \mathbf{m} by presenting the numerical results on the self-oscillation of \mathbf{m} in the two specific modes.

III. NUMERICAL RESULTS

A. $\mathbf{S} = S_0 \mathbf{m}_z$ (mode I)

In this case, \mathbf{S} applies along the z axis and \mathbf{h}_{ex} applies along the $\pm x$ axis, where Γ_1 and Γ_2 push \mathbf{m} toward the x - y plane while the torque due to \mathbf{S} prefers \mathbf{m} along the z axis. The stable self-oscillation of \mathbf{m} over broad ranges of h_x and S_0 can be realized and is shown below. Here we choose $h_x = 2.5 \text{ kOe}$ ($h_y = h_z = 0$) and $S_0 = 120 \text{ Oe}$, under which a perfectly periodic oscillation of $\mathbf{m}(t)$ is shown in Figs. 2(a) and 2(b). The amplitudes of components m_y and m_z are close to 1.0 but that for m_x is only ~ 0.3 , indicating that the precession of \mathbf{m} proceeds mainly on the y - z plane with a precession frequency of 8.58 GHz. This frequency can be modulated as required by adjusting h_x and S_0 . The curve (red and dashed curve) in Fig. 2(a) shows the evolution of $E(t)$ [Eq. (3)].¹³ The periodic oscillation of $E(t)$ is also an indication of the

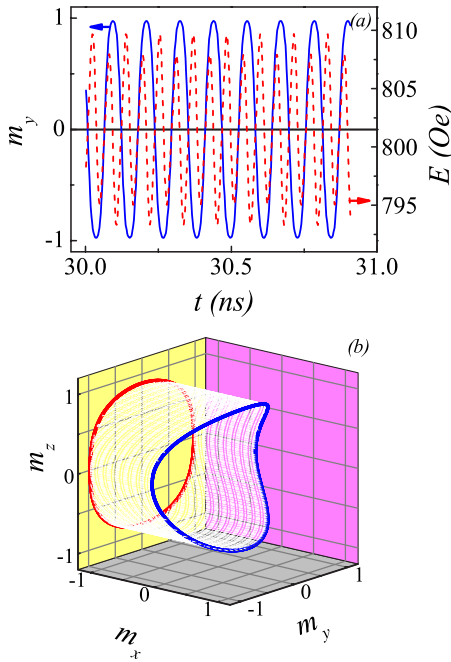


FIG. 2. (Color online) (a) Oscillation of magnetization component m_y (blue solid curve) and free energy E (red dashed curve) with time t . (b) Spatial trajectory of magnetization \mathbf{m} (blue color curve) and the projection of the trajectory on the y - z plane (red color curve).

self-oscillation of \mathbf{m} , revealing the negative feedback mechanism and the exact balance between the energy pumped by S and the damping dissipation loss.

The stable self-oscillation of $\mathbf{m}(t)$ can be further illustrated by evaluating the stability of the trajectory $\mathbf{m}(t)$ in the (θ, φ) state space. The immediate fixed point is point $P = (\pi/2, 0)$. The real part of the eigenvalue for the trajectory within a finite region around point P is $Z = S_0 - \alpha(2h_x + h_{de} + h_k)$, indicating that point P is a stable focus if $Z < 0$ and unstable focus if $Z > 0$. Thus, $Z \geq 0$ is the necessary condition for the existence of a limit cycle around point P .²⁴ For the present case ($h_x = 2.5$ kOe and $S_0 = 120$ Oe), $Z = 15$, indicative of no stable fixed point available in this finite region, while, on the other hand, there must exist at least one limit cycle as the generic attractor to the trajectories. For other regions far from point P in the (θ, φ) state space, nevertheless, the trajectory evolution has to be evaluated by numerical calculation using the fourth-order Runge-Kutta algorithm. The numerical results are summarized in Fig. 3. The entire (θ, φ) state space can be divided into two regions. All trajectories starting from a point within the central region (light magenta, region I) around point P will be attracted toward the limit cycle (blue line, indicated by the arrow), which corresponds to the highly stable self-oscillation of $\mathbf{m}(t)$. The other region (yellow, region II) is facilitated with four stable fixed points (red), A , B , C , and D . Any trajectory in this region will eventually evolve into one of the four fixed points.

The existence of the limit cycle and the stability of the fixed points in the (θ, φ) state space depend on the magnitude of the field terms, h_{ex} , h_{de} , h_k . Here we address the effect

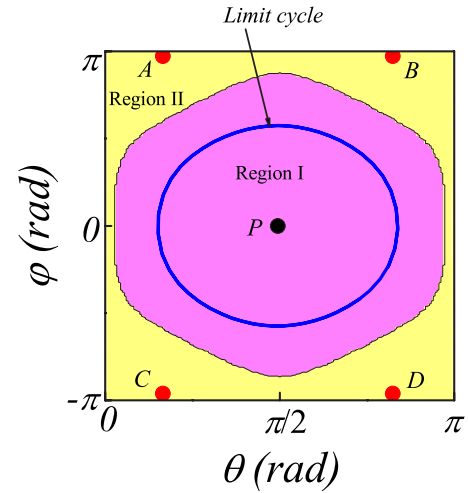


FIG. 3. (Color online) Stability diagram of the trajectory evolution in the θ - φ state space. The phase boundary divides the state space into two regions. Region I (magenta color) represents the steady-state precessional mode with the limit cycle (blue color, indicated by the arrow). Region II (yellow region) in the corners is the area of static-state mode with the four fixed points A , B , C , and D (red color). The coordinates for the four fixed points are $A = (\pi/6, 0.992\pi)$, $B = (5\pi/6, 0.992\pi)$, $C = (\pi/6, -0.992\pi)$, and $D = (5\pi/6, -0.992\pi)$, respectively.

of terms h_{ex} and h_{de} on the stability diagram (Fig. 3), noting that h_k is negligible compared with the other two fields. For example, when h_x and h_{de} are large, $Z < 0$ is obtained, indicating that point P is a stable focus, accompanied with the disappearance of the limit cycle. Consequently, the stability diagram of the trajectory evolution in the h_x - h_{de} plane can be evaluated, as shown in Fig. 4 with $S_0 = 120$ Oe, where four different stability regions are displayed. In region I, the limit cycle is the only stable attractor over the entire (θ, φ) state space, while for region II, both the limit cycle and the four fixed points (A, B, C, D) are locally stable (as shown in Fig. 3). In region III, only the four fixed points remain stable. For

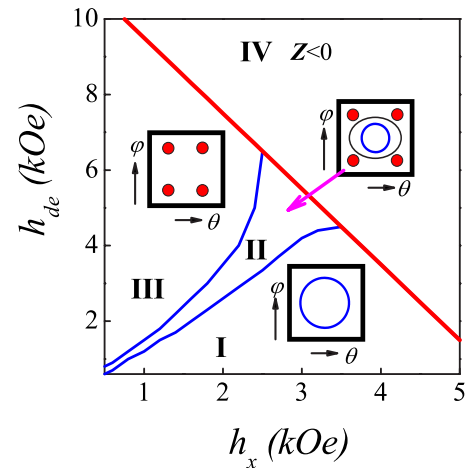


FIG. 4. (Color online) Stability diagram of the trajectory evolution in the (h_x, h_{de}) parameter plane. The three insets represent the schematic stability diagrams in the θ - φ state space corresponding to regions I, II, and III, respectively.

region IV, $Z < 0$, indicative of stable focus point P . The straight line separating region IV from the other regions is defined by $Z=0$ (bifurcation line), at which point P is marginally stable. Because no limit cycle is available in region IV, we pay no more attention to the stability of possible fixed points in this region. Here, it should be mentioned that for the sake of the self-oscillation of $\mathbf{m}(t)$, the system must be operated inside region I or II, and it is better to operate inside region I rather than inside region II, so that the trajectory of $\mathbf{m}(t)$ will evolve onto the limit cycle. One may also conclude that h_{de} should be chosen properly for the self-oscillation of $\mathbf{m}(t)$.

The role of S_0 should be addressed, too. If S_0 is small, the damping term may overcome the S -induced spin torque and eventually enforce the magnet toward the direction of the effective field [for case (a), the lower limit for S_0 is 105 Oe, at which $Z=0$]. This corresponds to shrinking of the limit cycle into point P in the (θ, φ) state space. If S_0 is large [in case (a), the upper limit is $S_0=127$ Oe], the S -induced spin torque will drive the magnet to one of the four stable fixed points (A, B, C, D). For simplicity, we consider a magnet in the case of $\alpha=0$, $h_{de}=h_k=0$. After the initial periods of transition, \mathbf{m} will move toward the y - z plane ($m_x=0$), and the final motion is governed by

$$\frac{1}{\gamma} \frac{d\theta}{dt} = S_0 \cos(\theta) \sin(\theta) + h_x. \quad (4)$$

When $|S_0 \cos(\theta) \sin(\theta) + h_x| > 0$, Eq. (4) yields a steady oscillation solution, which requires $2S_0 h_x$. Otherwise, \mathbf{m} of the nanomagnet will settle back into one of the stable fixed points. Moreover, if we include the damping term, S_0 should be larger than a critical value, or the spin torque cannot balance the damping motion.

B. $S=S_0(-m_z)$ (mode II)

For this case, as discussed previously, \mathbf{h}_{ex} is applied along the $\pm z$ axis and the spin torque will draw \mathbf{m} toward the x - y plane. Thus, the self-oscillation on the x - y plane is sustained. As an example, take $h_{ex}=1.5$ kOe and $S_0=500$ Oe. The calculated results are shown in Figs. 5(a) and 5(b). Again, the self-oscillation of \mathbf{m} is revealed, and it is seen that the amplitude of $m_z(t)$ is much smaller than that of $m_y(t)$ or $m_x(t)$, indicating that the oscillation proceeds almost on the x - y plane. If S_0 increases, m_z will be suppressed even more and tends to change toward zero. The self-oscillation frequency here is 4.3 GHz, almost the same as the frequency for the case of no damping. The tiny difference is due to the weak magnetic anisotropy along the y axis.

Similarly, the self-oscillation corresponds to the limit cycle [blue line, indicated by the arrow in Fig. 5(c)] in the (θ, φ) state space, which is different from that for case (a). In this case, the fixed point on line $\theta=0$ is unstable due to $Z=S_0+\alpha(h_{de}-h_z-h_k)>0$. As illustrated in Fig. 5(c), the allowed change of θ is small with respect to the variation of φ for the sake of the self-oscillation. If S is extremely high, $\theta=\pi/2$, it is characterized by a straight limit cycle. In the same way as in case (a), we analyze the trajectory stability of

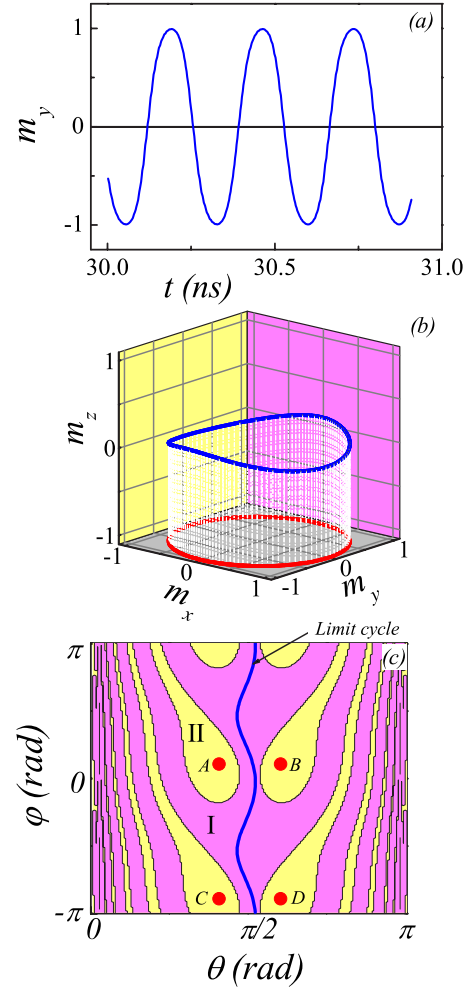


FIG. 5. (Color online) (a) Oscillation of magnetization component m_y with time t . (b) Spatial trajectory of magnetization \mathbf{m} (blue color curve) and the projection of the trajectory on the x - y plane (red color curve). (c) Stability diagram in the θ - φ state space. Region I (magenta) is the area of steady-state precessional mode. The blue curve as indicated by the arrow in this area is the limit cycle. Region II (yellow) belongs to the static-state mode area with the four fixed points (red). The four stable points are $A=(0.408\pi, 0.104\pi)$, $B=(0.598\pi, 0.104\pi)$, $C=(0.408\pi, -0.896\pi)$, and $D=(0.598\pi, -0.896\pi)$, respectively.

$\mathbf{m}(t)$ over the entire (θ, φ) state space and the results are shown in Fig. 5(c) where region II (light yellow) corresponds to the stationary mode and region I (light magenta) refers to the steady-state precession model. For the former mode, \mathbf{m} eventually evolves toward the four stable fixed points (A, B, C , and D , red color), while for the latter mode \mathbf{m} converges toward the limit cycle (indicated by the arrow), i.e., the self-oscillation of $\mathbf{m}(t)$. It is seen that the boundary between the two regions exhibits a complicated pattern and the two regions are single connected, because φ varies periodically in space. It should be mentioned that the stability pattern in the (θ, φ) state space is also dependent on \mathbf{h}_{ex} and \mathbf{h}_{de} , similar to case (a).

For both cases (modes I and II), S is applied along the z axis and the effect of spin torque is twofold: it balances Γ_1

and Γ_2 and helps stabilize the self-oscillation through the negative feedback mechanism. In fact, S can be applied along other directions and the self-oscillation of m may be excited, too. However, the negative feedback due to the spin torque may not be sufficient due to the large demagnetization field in the z axis. For instance, if both S and h_{ex} are applied along the x axis [$S=S_0(-m_x)$], the self-oscillation of m does occur, but it does not belong to mode II because the spin torque cannot effectively restrict m around the y - z plane and the negative feedback mechanism fails. The calculation shows that m follows some specific trajectories in the region $m_x > 0$. This self-oscillation is sensitive to h_{ex} and the system parameters, and can be classified into the limit cycle mode discussed in Ref. 13.

We have presented the two specific configurations for the self-oscillation of m upon the self-controlled SP current perpendicular (mode I) and parallel to h_{ex} (mode II), respectively. Upon different applications, the self-oscillation behavior can be easily manipulated by adjusting h_{ex} and S . This property has great significance for practical applications in terms of precise controlling of the self-oscillation, including the frequency and orientation of the oscillation. What should be mentioned here is that the demagnetization field must be taken into account since it plays an essential role in the symmetry breaking of the system.

C. Remarks

The above calculation is restricted to the single-domain nanomagnets and only the theoretical analysis is implemented. Nevertheless, the mutual controlling mechanism of $m(t)$ and S seems to be an effective approach to achieve the self-oscillation of m , and this self-control approach can be extended to other magnetic nanostructures and used to excite some dynamics behaviors, such as a magnetic vortex oscillation in nonuniform nanomagnets²⁵ and domain-wall motion in magnetic nanowires.²⁶ Even for the single-domain model, a lot of problems still exist. We will further study the manipulation of the oscillation frequency and the exact magnetic field dependence of the SP current, as well as the stability of limit cycles taking various kinds of noises into account.

For experimental realization of the two self-oscillation modes, some difficulties such as how to enable the SP current to synchronize with the variation of m may make the experiments challenging. In fact, a detailed calculation indi-

cates that the self-oscillation can be realized (in some cases) even for a constant SP current, as long as its direction is aligned accordingly. In the spin-valve language, it means that the direction of the SP current is controlled by the magnetic state of a free layer, which can flip between the parallel and antiparallel orientations with respect to the fixed layer. These two states are detected by a voltage change across the spin valve due to the giant magnetoresistance effect.¹⁵ A logic gate can be integrated with the valve circuit to detect the voltage change and thus manipulate the direction of SP current.

As for controlling the magnitude of the SP current, a simple and convenient approach seems to be not available to us at this moment, although quite a few complicated designs for detecting the z -axis component of the magnetization can be proposed, such as anisotropic magnetoresistance unit, which can be used to detect the value of m_z . Once m_z is measured, the SP current with $S \sim m_z$ or $S \sim -m_z$ can be applied to control the oscillation of m . It should be mentioned here that this feedback is not synchronous but delayed with respect to the variation of m . However, our calculation indicates that such a delay does not matter as long as this delay is much shorter than the period of the self-oscillation of m .

IV. CONCLUSION

In conclusion, the self-controlled spin-polarized current has been brought forward to excite the steady oscillation of magnetization in a nanomagnet. The basic idea is to employ the negative feedback model, which is realized by pumping the energy into the magnet using dynamical modulation of the spin-polarized current. The two special cases with the different alignments for the spin-polarized current have been discussed and the steady precession states of the magnetization motion have been obtained. This self-oscillation corresponds to the limit cycle in the state space, whose existence depends significantly on the demagnetization field.

ACKNOWLEDGMENTS

This work was supported by the Natural Science Foundation of China (10674061 and 50332020), the National Key Projects for Basic Researches of China (2006CB921802), and the 111 Project of MOE of China (B07026). We thank D. J. Le Boeuf, H. Yu, and W. W. Lin for providing a useful discussion of these concepts.

*Author to whom correspondence should be addressed; liujm@nju.edu.cn

¹J. C. Slonczewski, J. Magn. Magn. Mater. **159**, L1 (1996).

²L. Berger, Phys. Rev. B **54**, 9353 (1996).

³S. Zhang, P. M. Levy, and A. Fert, Phys. Rev. Lett. **88**, 236601 (2002).

⁴A. Shpiro, P. M. Levy, and S. Zhang, Phys. Rev. B **67**, 104430 (2003).

⁵S. I. Kiselev, J. C. Sankey, I. N. Krivorotov, N. C. Emley, R. J.

Schoelkopf, R. A. Buhrman, and D. C. Ralph, Nature (London) **425**, 380 (2003).

⁶S. I. Kiselev, J. C. Sankey, I. N. Krivorotov, N. C. Emley, M. Rinkoski, C. Perez, R. A. Buhrman, and D. C. Ralph, Phys. Rev. Lett. **93**, 036601 (2004).

⁷I. N. Krivorotov, N. C. Emley, J. C. Sankey, S. I. Kiselev, D. C. Ralph, and R. A. Buhrman, Science **307**, 228 (2005).

⁸J. Z. Sun, Phys. Rev. B **62**, 570 (2000).

⁹Z. Li and S. Zhang, Phys. Rev. B **68**, 024404 (2003).

- ¹⁰D. V. Berkov and N. L. Gorn, Phys. Rev. B **72**, 094401 (2005).
- ¹¹K. J. Lee, A. Deac, O. Redon, Jean-Pierre Nozieres, and B. Dieny, Nat. Mater. **3**, 877 (2004).
- ¹²S. A. Wolf, D. D. Awschalom, R. A. Buhrman, J. M. Daughton, S. von Molnar, M. L. Roukes, A. Y. Chtchelkanova, and D. M. Treger, Science **294**, 1488 (2001).
- ¹³G. Bertotti, C. Serpico, I. D. Mayergoyz, A. Magni, M. d'Aquino, and R. Bonin, Phys. Rev. Lett. **94**, 127206 (2005).
- ¹⁴Z. Li, Y. C. Li, and S. Zhang, Phys. Rev. B **74**, 054417 (2006).
- ¹⁵W. H. Rippard, M. R. Pufall, S. Kaka, T. J. Silva, S. E. Russek, and J. A. Katine, Phys. Rev. Lett. **95**, 067203 (2005).
- ¹⁶S. Kaka, M. R. Pufall, W. H. Rippard, T. J. Silva, S. E. Russek, and J. A. Katine, Nature (London) **437**, 389 (2005).
- ¹⁷F. B. Mancoff, N. D. Rizzo, B. N. Engel, and S. Tehrani, Nature (London) **437**, 393 (2005).
- ¹⁸A. N. Slavin and V. S. Tiberkevich, Phys. Rev. B **74**, 104401 (2006).
- ¹⁹J. Grollier, V. Cros, and A. Fert, Phys. Rev. B **73**, 060409(R) (2006).
- ²⁰Z. Z. Sun and X. R. Wang, Phys. Rev. B **73**, 092416 (2006).
- ²¹C. Thirion, W. Wernsdorfer, and D. Mailly, Nat. Mater. **2**, 524 (2003).
- ²²B. Hillebrands and A. Thiaville, *Spin Dynamics in Confined Magnetic Structures III* (Springer, Berlin, 2005).
- ²³Here, \mathbf{S} is the spin-polarized current field instead of the current itself. S is summarized as the overall coefficient of the spin torque.
- ²⁴Ferdinand Verhulst, *Nonlinear Differential Equations and Dynamical Systems* (Springer, New York, 2003); S. Wiggins, *Introduction to Applied Nonlinear Dynamical Systems and Chaos* (Springer, New York, 1990).
- ²⁵V. S. Pribiag, I. N. Krivorotov, G. D. Fuchs, P. M. Braganca, O. Ozatay, J. C. Sankey, D. C. Ralph, and R. A. Buhrman, Nat. Phys. **3**, 498 (2007).
- ²⁶L. Thomas, M. Hayashi, X. Jiang, R. Moriya, C. Rettner, and S. Parkin, Science **315**, 1553 (2007).